


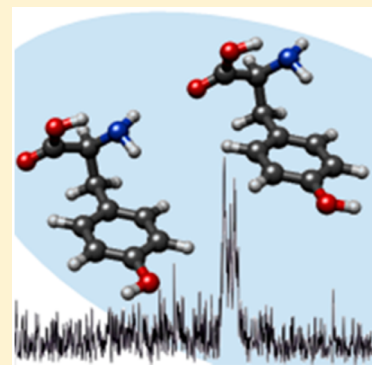
# 1 The Rotational Spectrum of Tyrosine

2 Cristóbal Pérez,<sup>†</sup> Santiago Mata, Carlos Cabezas, Juan C. López, and José. L. Alonso\*

3 Grupo de Espectroscopia Molecular (GEM), Edificio Quifima, Laboratorios de Espectroscopia y Biospectroscopia, Unidad Asociada  
4 CSIC, Parque Científico Uva, Universidad de Valladolid, 47011 Valladolid, Spain

5  Supporting Information

6 **ABSTRACT:** In this work neutral tyrosine has been generated in the gas phase by laser  
7 ablation of solid samples, and its most abundant conformers characterized through their  
8 rotational spectra. Their identification has been made by comparison between the  
9 experimental and *ab initio* values of the rotational and quadrupole coupling constants.  
10 Both conformers are stabilized by an O–H•••N hydrogen bond established within the  
11 amino acid skeleton chain and an additional weak N–H••• $\pi$  hydrogen bond. The  
12 observed conformers differ in the orientation of the phenolic –OH group.



## 13 ■ INTRODUCTION

14 Proteinogenic amino acids are indispensable agents of bio-  
15 logical function since they constitute the building blocks of  
16 peptides and proteins. In addition they may have nonprotein  
17 functions as neurotransmitters or being precursors of important  
18 neurotransmitters or hormones. The function of proteins and  
19 their multidimensional structure are highly dependent upon the  
20 conformation that their constituent amino acids may adopt.  
21 The knowledge of the structure and conformational behavior of  
22 those building blocks is thus an important question not only to  
23 biochemistry but also for chemistry, since those flexible  
24 molecules constitute structural models to study the inter-  
25 molecular forces that control molecular conformation. The  
26 advantage of gas-phase conformational studies lies in the  
27 opportunity to obtain the intrinsic properties of the amino acids  
28 in isolation, free of the intermolecular interactions which occur  
29 in condensed phases where amino acids are bipolar zwitterionic  
30 species. Electronic spectroscopy techniques such as high  
31 resolution laser-induced fluorescence (LIF) or resonance  
32 enhanced multiphoton ionization (REMPI) in combination  
33 with supersonic jets have been used to elucidate the structures  
34 of gas phase proteogenic amino acids bearing chromophore  
35 groups. Hence, these techniques have been applied to tyrosine  
36 (Tyr), tryptophan (Trp), and phenylalanine (Phe), which were  
37 the subject of a large number of investigations.<sup>1–18</sup> REMPI and  
38 LIF experiments on Tyr<sup>12–15</sup> reported up to ten vibronic bands  
39 which suggested the presence of a large number of stable  
40 conformers. More recently, eight different structures of Tyr  
41 were confirmed by using UV–UV and IR–UV hole burning  
42 techniques.<sup>16,17</sup> In a last work, using the same experimental  
43 approach, Shimozono et al.<sup>18</sup> interpreted the jet cooled  
44 electronic spectra on the basis of 12 different conformers.

45 Microwave spectroscopy is particularly well adapted to the  
46 study of multiconformer systems such as amino acids, since it  
47 has an inherently high resolution and is exceptionally sensitive  
48 to molecular geometry and mass distribution changes and it is  
49 not constrained by the need for a chromophore group.  
50 However, the vaporization of solid biomolecules imposed  
51 serious limitations to study high melting compounds such as  
52 amino acids which easily decompose by classical heating  
53 methods. Recent developments in laser ablation techniques  
54 have allowed us to overcome vaporization problems. In  
55 particular, combining Fourier transform microwave spectro-  
56 scopy with laser ablation techniques in a supersonic expansion  
57 (LA-MB-FTMW)<sup>19–21</sup> has provided a new approach to the  
58 structural studies of amino acids. Apart from glycine<sup>22,23</sup> and  
59 alanine,<sup>24</sup> first studied by classical heating methods, a large  
60 number of proteogenic and nonproteogenic aliphatic amino  
61 acids<sup>19–21,25–34</sup> have been studied by the above technique.  
62 Their applicability to aromatic amino acids was first tested in  
63 phenylglycine<sup>35</sup> and latter applied to the studies of Phe<sup>36</sup> and  
64 Trp.<sup>37</sup> Significant photofragmentation was detected, and  
65 consequently, our experimental setup was modified trying to  
66 minimize it. Shorter laser pulses (30 ps length pulse) and  
67 shorter wavelengths (Nd:YAG 355 nm) have been recently  
68 implemented in our new instrumentation<sup>37,38</sup> in order to  
69 minimize photofragmentation processes. In the context of our  
70 ongoing investigation of the conformational panorama of  
71 amino acids using rotational spectroscopy, we report in this  
72 paper the first rotational study of the proteogenic aromatic  
73 amino acid tyrosine.

Received: February 24, 2015

Revised: March 31, 2015

Table 1. Experimental Spectroscopic Parameters for the Observed Conformers IIa1 and IIa2 of L-Tyrosine

Parameter <sup>a</sup>	Experimental		Theory	
	Rotamer X	Rotamer Y	Conformer IIa1	Conformer IIa2
A	1529.6791(40) <sup>b</sup>	1525.2543(29)	1519.5	1516.4
B	463.94021(32)	465.48173(25)	472.6	474.2
C	425.76168(40)	427.31023(27)	433.2	434.8
$\Delta_J$	0.0507(29)	0.0527(19)		
$\chi_{aa}$	0.709(14)	0.740(15)	0.94	0.96
$\chi_{bb}$	0.236(88)	0.247(92)	-0.29	-0.28
$\chi_{cc}$	-0.945(88)	-0.988(92)	-0.64	-0.67

<sup>a</sup>A, B, and C are the rotational constants;  $\Delta_J$  is the quartic centrifugal distortion constant;  $\chi_{aa}$ ,  $\chi_{bb}$ , and  $\chi_{cc}$  are the diagonal elements of the <sup>14</sup>N nuclear quadrupole coupling tensor. <sup>b</sup>Standard error in parentheses in units of the last digit.

## 74 ■ EXPERIMENTAL SECTION

75 The rotational spectrum of Tyr was observed using a new laser  
76 ablation molecular beam Fourier transform microwave (LA-  
77 MB-FTMW)<sup>20,21,38</sup> spectrometer operating in the 4–10 GHz  
78 frequency range. Solid rods of fine-powdered tyrosine (mp  
79 290–295 °C) were mixed with minimum quantities of a  
80 commercial binder to form a cylindrical rod. The samples were  
81 then vaporized using the third harmonic (355 nm) of a  
82 Nd:YAG picosecond laser (30 ps length pulse) using energies  
83 of ~2 mJ/pulse. The neutral vaporized molecules were seeded  
84 in the carrier gas (Ne, 15 bar) and expanded into a Fabry-Pérot  
85 resonator. After sending the microwave pulses through the  
86 cavity, the emission FID (free induction decay) of the  
87 molecules was recorded in the time-domain and Fourier  
88 transformed to yield the frequency-domain spectrum. Since the  
89 supersonic jet and the microwave resonator axis are collinearly  
90 placed, signals appeared split into Doppler doublets. The  
91 arithmetic mean of the doublets was taken as the final  
92 frequency. The estimated accuracy of the frequency measure-  
93 ments is better than 3 kHz.

## 94 ■ RESULTS AND DISCUSSION

95 Before starting the experimental study, we extended the  
96 previous *ab initio* calculations<sup>39</sup> on the low energy conformers  
97 of Tyr to predict the rotational and nuclear quadrupole  
98 coupling constants as well as electric dipole moment  
99 components which are needed for the interpretation of the  
100 rotational spectrum. Geometry optimizations were carried out  
101 with the Gaussian suite of programs<sup>40</sup> using second-order  
102 Møller–Plesset perturbation theory (MP2) in the frozen-core  
103 approximation and Pople's 6-311++G(d,p) basis set. This level  
104 of theory has proven to give very good results for the rotational  
105 parameters at a reasonable computational cost.<sup>19–33</sup> The  
106 calculated spectroscopic parameters for the ten lowest-energy  
107 conformers of Tyr are shown in Table S1 of the Supporting  
108 Information.

109 All conformers are predicted to be near-prolate asymmetric  
110 tops with a nonzero  $\mu_a$  component of the electric dipole  
111 moment. In this way, their R-branch,  $\mu_a$ -type spectra are  
112 expected to show the characteristic patterns consisting of  
113 groups of lines separated by approximately  $B + C$ . Initially, the  
114 polarization power was set to optimally polarize the transitions  
115 associated with moderate values of  $\mu_a$ . Hence, we were able to  
116 detect two sets of weak  $\mu_a$ -type R-branch series transitions,  
117 attributable to two different rotamers which initially were  
118 labeled as X and Y. The subsequent fitting and prediction  
119 iterative procedure allows us to observe new  $\mu_a$  transitions and  
120 to extend our measurements to the R-branch  $\mu_b$ -type spectrum.

All the observed transitions (see Figure S1 and Table S3 and S4  
of the Supporting Information) were split into several close  
hyperfine components showing the characteristic pattern due to  
a <sup>14</sup>N nucleus, which confirms the presence of a single nitrogen  
atom in the observed species. This hyperfine structure arises  
from the interaction of the electric quadrupole moment of the  
<sup>14</sup>N ( $I = 1$ ) nucleus with the electric field gradient created at the  
site of the quadrupolar nucleus by the rest of the electronic and  
nuclear charges of the molecule. This interaction gives rise to  
the coupling of the <sup>14</sup>N nuclear spin with the overall angular  
momentum, which results in a characteristic hyperfine structure  
observable in the rotational spectra. The associated spectro-  
scopic parameters are the quadrupole coupling constants  $\chi_{\alpha\beta}$   
( $\alpha\beta = a, b, c$ ). These are the elements of the quadrupole  
coupling tensor  $\chi$ , which is related to the electric field gradient  
tensor  $q$  by  $\chi = eQq$ , where  $eQ$  is the electric quadrupole  
moment. According to this, the spectra were analyzed<sup>41</sup> using  
the semirigid rotor Hamiltonian of Watson in the A reduction  
and the I' representation  $H_R^{(A)}$ ,<sup>42</sup> supplemented with a term to  
take into account the quadrupole interaction  $H_Q$ ,<sup>43</sup> namely  $H =$   
 $H_R^{(A)} + H_Q$ . The analysis allowed the determination of the  
rotational constants, the centrifugal distortion constant  $\Delta_J$ , and  
the diagonal elements of the quadrupole coupling tensor for  
both X and Y rotamers (see Table 1).

The comparison of the experimental and predicted rotational  
parameters in Table 1 shows that the observed rotational  
constants are in good agreement with those predicted for  
conformers IIa1 and IIa2 (collected also in Table 1 for  
comparison). The same conclusion can be reached from the  
comparison of the values of the <sup>14</sup>N quadrupole coupling  
constants. The experimental values are only in good agreement  
with those predicted for conformers IIa1 and IIa2. The values  
of the <sup>14</sup>N quadrupole coupling constants are very sensitive to  
the orientation of the -NH<sub>2</sub> group with respect to the principal  
inertial axis system so that in most cases these constants led to a  
conclusive assignment of the observed conformers. However, in  
this case, conformers IIa1 and IIa2 have practically the same  
values of the <sup>14</sup>N quadrupole coupling constants because the  
rotation of the principal inertial axis system induced by the  
change in the structure of the phenolic -OH group does not  
contribute to significant changes in the quadrupole coupling  
constants. Therefore, it is not possible to carry out an  
unequivocal assignment of both observed rotamers on the  
basis of these constants. Fortunately, the change in orientation  
of the -OH group in conformers IIa1 and IIa2 causes  
distinctive shifts in the inertial moments which are translated to  
the rotational constants. Thus, the small shifts in the rotational  
constants do have the key to discern between both conformers.  
The changes in the experimental values of the rotational

170 constants between rotamers X and Y are  $\Delta A = \Delta A_Y - \Delta A_X \approx$   
 171  $-4.4$  MHz,  $\Delta B \approx 1.5$  MHz and  $\Delta C \approx 1.5$  MHz. These values  
 172 are in good agreement with the differences between the  
 173 rotational constants of conformers IIa1 and IIa2;  $\Delta A = \Delta A_{IIa2}$   
 174  $- \Delta A_{IIa1} \approx -3.1$  MHz,  $\Delta B \approx 1.6$  MHz, and  $\Delta C \approx 1.6$  MHz.  
 175 This fact allows the identification of rotamers X and Y as the  
 176 lowest lying energy conformers IIa1 and IIa2, respectively. The  
 177 small discrepancy found between the experimental and  
 178 predicted values of quadrupole coupling constants (Table 1)  
 179 is due to a slight variation in the actual orientation of the amino  
 180 group with respect to that predicted via ab initio methods.  
 181 Hence, when the amino group rotated ( $6^\circ$  on the dihedral  
 182 angle  $\angle\text{HNCC}$ ) from the equilibrium value, the predicted and  
 183 experimental values of the nuclear quadrupole coupling  
 184 constants are nearly in coincidence (see Table S2).

185 In the next stage of our investigation, we focused the  
 186 experimental searches to detect spectral signatures of Ia and IIb  
 187 conformers, predicted higher in energy. We observed sets of  
 188 very weak  $\mu_a$ -type R-branch rotational transitions in the  
 189 predicted frequency intervals for conformers IIb1 and IIb2,  
 190 predicted to have high values of the  $\mu_a$  electric dipole moment  
 191 component. We were only able to observe a few lines of each  
 192 set with a non-well-resolved hyperfine structure; no spectro-  
 193 scopic constants could be derived. After performing wide scans  
 194 with different experimental conditions, no lines attributable to  
 195 other conformers of Tyr were observed.

196 The two observed conformers of Tyr shown in Figure 1 are  
 197 stabilized by an O–H $\cdots$ N hydrogen bond with a COOH trans

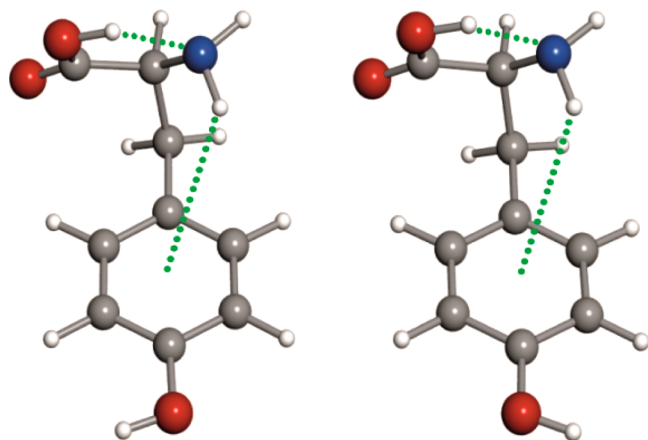


Figure 1. 3D structures of observed conformers (IIa1(left) and IIa2 (right)) of Tyr showing the intramolecular interactions which stabilize both structures.

198 configuration (type II of the amino acids<sup>20</sup>). Moreover, one of  
 199 the hydrogen atoms of the amino group is pointing toward the  
 200  $\pi$  electron density of the ring, indicating the existence of an N–  
 201 H $\cdots\pi$  interaction. The modified orientation of the amino group  
 202 mentioned above points to the establishment of this N–H $\cdots\pi$   
 203 interaction by decreasing the hydrogen bond distance. Both  
 204 intramolecular hydrogen bonds form a chain that reinforces  
 205 their strength through cooperative effects.<sup>44,45</sup> For the over-  
 206 whelming majority of the  $\alpha$ -amino acids studied so far, a type I  
 207 conformer has been found as global minimum. A few  
 208 exceptions have been found for which a type II conformer  
 209 has been found to be the most stable conformer. Those include  
 210 the imino acids proline,<sup>19,32</sup> and hydroxyproline,<sup>28</sup> asparagine,<sup>34</sup>  
 211 phenylalanine,<sup>36</sup> tryptophan,<sup>37</sup> and histidine.<sup>38</sup> With the

exception of proline and hydroxyproline, the type II O–H $\cdots$  212  
 N hydrogen bond established within the amino acid backbone 213  
 is reinforced by an additional bond from the amino group to 214  
 the lateral chain in all cases. In the case of the phenylalanine,<sup>36</sup> 215  
 tryptophan,<sup>37</sup> and tyrosine, this additional interaction corre- 216  
 sponds to a weak N–H $\cdots\pi$  weak hydrogen bond. 217

Relative intensity measurements on selected  $\mu_a$ -type lines of 218  
 the IIa1 and IIa2 conformers indicate that the relative 219  
 populations follow the order IIa2 > IIa1, in agreement with 220  
 the theoretically predicted relative energies. This pair of 221  
 conformers, which differ only in the OH arrangement, have a 222  
 predicted energy difference of  $132\text{ cm}^{-1}$ . This energy difference 223  
 could be tentatively explained by the existence of local dipole– 224  
 local dipole<sup>46</sup> interaction between the amino acid group and the 225  
 side chain ( $-\text{CH}_2-\text{C}_6\text{H}_4-\text{OH}$ ). These dipoles find a more 226  
 favorable arrangement for conformer IIa2, increasing in this 227  
 way the relative stability of this conformer. 228

In conclusion, we have observed two conformers of Tyr 229  
 through the analysis of its rotational spectrum. These 230  
 conformers are stabilized by O–H $\cdots$ N and N–H $\cdots\pi$  hydrogen 231  
 bond interactions and derive from the most stable forms 232  
 observed for the related amino acid Phe.<sup>36</sup> The weakness of the 233  
 spectrum and the low number of observed conformers for Tyr 234  
 compared with those detected for aliphatic amino acids<sup>30–33</sup> 235  
 can be attributable to photofragmentation/ionization processes 236  
 during the laser ablation course. As reported for Phe,<sup>47</sup> 237  
 ionization processes would favor the presence of only IIa and 238  
 IIb conformers, with higher ionization energy, in the supersonic 239  
 jet. We have monitored photofragmentation effects using a 240  
 time-of-flight mass spectrometer (TOF-MS) coupled with the 241  
 same laser ablation nozzle used in our LA-MB-FTMW 242  
 experiment and we found (See Figure S2 of the Supporting 243  
 Information) a large amount of Tyr fragments, indicating that 244  
 photofragmentation of Tyr occurs to a large extent in the 245  
 ablation process. The subsequent depletion of the number 246  
 density of tyrosine in the supersonic expansion would cause the 247  
 observation of weaker spectra. Despite the important improve- 248  
 ments recently achieved in the observation of nucleoside 249  
 uridine,<sup>48</sup> the intrinsic effects of photofragmentation associated 250  
 with the aromatic amino acids make extremely difficult the 251  
 observation of their complete conformational panorama. 252

## ■ ASSOCIATED CONTENT

### 📄 Supporting Information

Complete ref 40, predicted ab initio molecular properties for 255  
 the lower-energy conformers of the tyrosine together with 256  
 MP2/6-311++G(d,p) equilibrium principal axis coordinates, 257  
 quadrupole coupling constants calculated at the different 258  
 dihedral angles  $\angle\text{HNCC}$  for the observed conformers, 259  
 observed rotational transitions for the two detected conformers, 260  
 and list of measured transitions and mass spectrum of tyrosine. 261  
 This material is available free of charge via the Internet at 262  
<http://pubs.acs.org>. 263

## ■ AUTHOR INFORMATION

### Corresponding Author

\* E-mail: jalonso@qf.uva.es Phone: +34 983186348 Fax: +34 266  
 983186349. 267

### Present Address

†(C.P.) Max-Planck Institute for the Structure and Dynamics of 269  
 Matter; Luruper Chaussee 149, D-22761 Hamburg. Germany. 270



271 **Notes**

272 The authors declare no competing financial interest.

273 **ACKNOWLEDGMENTS**

274 This research was supported by Ministerio de Ciencia e  
275 Innovación (grant numbers CTQ 2010-19008, CTQ 2013-  
276 40717-P, and Consolider Ingenio 2010 CSD 2009-00038) and  
277 Junta de Castilla y León (grant number VA175U13). C.C.  
278 thanks the Junta de Castilla y León for the postdoctoral  
279 contract (grant number CIP13/01).

280 **REFERENCES**

- 281 (1) Philips, L. A.; Webb, S. P.; Martinez, S. J.; Fleming, G. R.; Levy,  
282 D. H. Time-Resolved Spectroscopy of Tryptophan Conformers in a  
283 Supersonic Jet. *J. Am. Chem. Soc.* **1988**, *110*, 1352–1355.
- 284 (2) Rizzo, T. R.; Park, Y. D.; Peteanu, L. A.; Levy, D. H. The  
285 Electronic Spectrum of the Amino Acid Tryptophan in the Gas Phase.  
286 *J. Chem. Phys.* **1986**, *84*, 2534–2541.
- 287 (3) Cable, J. R.; Tubergen, M. J.; Levy, D. H. Laser Desorption  
288 Molecular Beam Spectroscopy: The Electronic Spectra of Tryptophan  
289 Peptides in the Gas Phase. *J. Am. Chem. Soc.* **1987**, *109*, 6198–6199.
- 290 (4) Snoek, L. C.; Kroemer, R. T.; Hockridge, M. R.; Simons, J. P.  
291 Conformational Landscapes of Aromatic Amino Acids in the Gas  
292 Phase: Infrared and Ultraviolet Ion Dip Spectroscopy of Tryptophan.  
293 *Phys. Chem. Chem. Phys.* **2001**, *3*, 1819–1826.
- 294 (5) Snoek, L. C.; Kroemer, R. T.; Simons, J. P. A Spectroscopic and  
295 Computational Exploration of Tryptophan–Water Cluster Structures  
296 in the Gas Phase. *Phys. Chem. Chem. Phys.* **2002**, *4*, 2130–2139.
- 297 (6) Martinez, S. J., III; Alfano, J. C.; Levy, D. H. The Electronic  
298 Spectroscopy of Tyrosine and Phenylalanine Analogs in a Supersonic  
299 Jet: Acidic Analogs. *J. Mol. Spectrosc.* **1991**, *145*, 100–111.
- 300 (7) Snoek, L. C.; Robertson, E. G.; Kroemer, R. T.; Simons, J. P.  
301 Conformational Landscapes in Amino Acids: Infrared and Ultraviolet  
302 Ion-Dip Spectroscopy of Phenylalanine in the Gas Phase. *Chem. Phys.*  
303 *Lett.* **2000**, *321*, 49–56.
- 304 (8) Lee, K. T.; Sung, J.; Lee, K. J.; Kim, S. K.; Park, Y. D. Resonant  
305 Two-Photon Ionization Study of Jet-Cooled Amino Acid: L-Phenyl-  
306 alanine and Its Monohydrated Complex. *J. Chem. Phys.* **2002**, *116*,  
307 8251–8254.
- 308 (9) Lee, K. T.; Sung, J.; Lee, K. J.; Park, Y. D.; Kim, S. K.  
309 Conformation-Dependent Ionization Energies of L-Phenylalanine.  
310 *Angew. Chem., Int. Ed.* **2002**, *41*, 4114–4117.
- 311 (10) Hashimoto, T.; Takasu, Y.; Yamada, Y.; Ebata, T. Anomalous  
312 Conformer Dependent S1 Lifetime of L-Phenylalanine. *Chem. Phys.*  
313 *Lett.* **2006**, *421*, 227–231.
- 314 (11) Ebata, T.; Hashimoto, T.; Ito, T.; Inokuchi, Y.; Altunsoy, F.;  
315 Brutschy, B.; Tarakeshwar, P. Hydration Profiles of Aromatic Amino  
316 Acids: Conformations and Vibrations of L-phenylalanine–(H<sub>2</sub>O)<sub>n</sub>  
317 Clusters. *Phys. Chem. Chem. Phys.* **2006**, *8*, 4783–4791.
- 318 (12) Martinez, S. J., III; Alfano, J. C.; Levy, D. H. The Electronic  
319 Spectroscopy of the Amino Acids Tyrosine and Phenylalanine in a  
320 Supersonic Jet. *J. Mol. Spectrosc.* **1992**, *156*, 421–430.
- 321 (13) Martinez, S. J.; Alfano, J. C.; Levy, D. H. The Electronic  
322 Spectroscopy of Tyrosine and Phenylalanine Analogs in a Supersonic  
323 Jet: Basic Analogs. *J. Mol. Spectrosc.* **1993**, *158*, 82–92.
- 324 (14) Lindinger, A.; Toennies, J. P.; Vilesov, A. F. High Resolution  
325 Vibronic Spectra of the Amino Acids Tryptophan and Tyrosine in 0.38  
326 K Cold Helium Droplets. *J. Chem. Phys.* **1999**, *110*, 1429–1436.
- 327 (15) Grace, L. I.; Cohen, R.; Dunn, T. M.; Lubman, D. M.; de Vries,  
328 M. S. The R2PI Spectroscopy of Tyrosine: A Vibronic Analysis. *J. Mol.*  
329 *Spectrosc.* **2002**, *215*, 204–219.
- 330 (16) Inokuchi, Y.; Kobayashi, Y.; Ito, T.; Ebata, T. Conformation of  
331 L-Tyrosine Studied by Fluorescence-Detected UV–UV and IR–UV  
332 Double-Resonance Spectroscopy. *J. Phys. Chem. A* **2007**, *111*, 3209–  
333 3215.
- 334 (17) Abo-Riziq, A.; Grace, L.; Crews, B.; Callahan, M. P.; van  
335 Mourik, T.; de Vries, M. S. Conformational Structure of Tyrosine,

- Tyrosyl-glycine, and Tyrosyl-glycyl-glycine by Double Resonance  
Spectroscopy. *J. Phys. Chem. A* **2011**, *115*, 6077–6087. 336
- (18) Shimozono, Y.; Yamada, K.; Ishiuchi, S.; Tsukiyama, K.; Fujii,  
337 M. Revised Conformational Assignments and Conformational  
338 Evolution of Tyrosine by Laser Desorption Supersonic Jet Laser  
339 Spectroscopy. *Phys. Chem. Chem. Phys.* **2013**, *15*, 5163–5175. 341
- (19) Lesarri, A.; Mata, S.; Cocinero, E. J.; Blanco, S.; López, J. C.;  
342 Alonso, J. L. The Structure of Neutral Proline. *Angew. Chem., Int. Ed.*  
343 **2002**, *41*, 4673–4676. 344
- (20) Alonso, J. L.; Pérez, C.; Sanz, M. E.; López, J. C.; Blanco, S.  
345 Seven Conformers of L-Threonine in the Gas Phase: A LA-MB-  
346 FTMW Study. *Phys. Chem. Chem. Phys.* **2009**, *11*, 617–627. 347
- (21) Peña, I.; Sanz, M. E.; López, J. C.; Alonso, J. L. Preferred  
348 Conformers of Proteinogenic Glutamic Acid. *J. Am. Chem. Soc.* **2011**,  
349 *134*, 2305–2312. 350
- (22) Brown, R. D.; Godfrey, P. D.; Storey, J. W. V.; Bassez, M.-P.  
351 Microwave Spectrum and Conformation of Glycine. *J. Chem. Soc.,*  
352 *Chem. Commun.* **1978**, 547–548. 353
- (23) Suenram, R. D.; Lovas, F. J. Millimeter Wave Spectrum of  
354 Glycine. *J. Mol. Spectrosc.* **1978**, *72*, 372–382. 355
- (24) Godfrey, P. D.; Firth, S.; Hatherley, L. D.; Brown, R. D.; Pierlot,  
356 A. P. Millimeter-Wave Spectroscopy of Biomolecules: Alanine. *J. Am.*  
357 *Chem. Soc.* **1993**, *115*, 9687–9691. 358
- (25) Blanco, S.; Lesarri, A.; López, J. C.; Alonso, J. L. The Gas-Phase  
359 Structure of Alanine. *J. Am. Chem. Soc.* **2004**, *126*, 11675–11683. 360
- (26) Lesarri, A.; Cocinero, E. J.; López, J. C.; Alonso, J. L. The Shape  
361 of Neutral Valine. *Angew. Chem., Int. Ed.* **2004**, *43*, 605–610. 362
- (27) Lesarri, A.; Sánchez, R.; Cocinero, E. J.; López, J. C.; Alonso, J.  
363 L. Coded Amino Acids in Gas Phase: The Shape of Isoleucine. *J. Am.*  
364 *Chem. Soc.* **2005**, *127*, 12952–12956. 365
- (28) Lesarri, A.; Cocinero, E. J.; López, J. C.; Alonso, J. L. Shape of  
366 4(S)- and 4(R)-Hydroxyproline in Gas Phase. *J. Am. Chem. Soc.* **2005**,  
367 *127*, 2572–2579. 368
- (29) Cocinero, E. J.; Lesarri, A.; Grabow, J.-U.; López, J. C.; Alonso,  
369 J. L. The Shape of Leucine in the Gas Phase. *ChemPhysChem* **2007**, *8*,  
370 599–604. 371
- (30) Blanco, S.; Sanz, M. E.; López, J. C.; Alonso, J. L. Revealing the  
372 Multiple Structures of Serine. *Proc. Natl. Acad. Sci.* **2007**, *104*, 20183–  
373 20188. 374
- (31) Sanz, M. E.; Blanco, S.; López, J. C.; Alonso, J. L. Rotational  
375 Probes of Six Conformers of Neutral Cysteine. *Angew. Chem., Int. Ed.*  
376 **2008**, *47*, 6216–6220. 377
- (32) Mata, S.; Vaquero, V.; Cabezas, C.; Peña, I.; Pérez, C.; López, J.  
378 C.; Alonso, J. L. Observation of Two New Conformers of Neutral  
379 Proline. *Phys. Chem. Chem. Phys.* **2009**, *11*, 4141–4144. 380
- (33) Sanz, M. E.; López, J. C.; Alonso, J. L. Six Conformers of  
381 Neutral Aspartic Acid Identified in the Gas Phase. *Phys. Chem. Chem.*  
382 *Phys.* **2010**, *12*, 3573–3578. 383
- (34) Cabezas, C.; Varela, M.; Peña, I.; Mata, S.; López, J. C.; Alonso,  
384 J. L. The Conformational Locking of Asparagine. *Chem. Commun.*  
385 **2012**, 48, 5934–5936. 386
- (35) Sanz, M. E.; Cortijo, V.; Caminati, W.; López, J. C.; Alonso, J. L.  
387 The Conformers of Phenylglycine. *Chem.—Eur. J.* **2006**, *12*, 2564–  
388 2570. 389
- (36) Pérez, C.; Mata, S.; Blanco, S.; López, J. C.; Alonso, J. L. Jet-  
390 Cooled Rotational Spectrum of Laser-Ablated Phenylalanine. *J. Phys.*  
391 *Chem. A* **2011**, *115*, 9653–9657. 392
- (37) Sanz, M. E.; Cabezas, C.; Mata, S.; Alonso, J. L. Rotational  
393 Spectrum of Tryptophan. *J. Chem. Phys.* **2014**, *140*, 204308. 394
- (38) Bermúdez, C.; Mata, S.; Cabezas, C.; Alonso, J. L. Tautomerism  
395 in Neutral Histidine. *Angew. Chem., Int. Ed.* **2014**, *53*, 11015–11018. 396
- (39) Zhang, M.; Huang, Z.; Lin, Z. Systematic Ab Initio Studies of  
397 the Conformers and Conformational Distribution of Gas-Phase  
398 Tyrosine. *J. Chem. Phys.* **2005**, *122*, 134313. 399
- (40) Frisch, M. J.; Trucks, G. W.; Schlegel, H. B.; Scuseria, G. E.;  
400 Robb, M. A.; Cheeseman, J. R.; Montgomery, J. A., Jr.; Vreven, T.;  
401 Kudin, K. N.; Burant, J. C.; et al. GAUSSIAN 03 (Revision B.04) (See  
402 Supporting Information for full citation). 403

- 404 (41) Pickett, H. M. The Fitting and Prediction of Vibration-Rotation  
405 Spectra with Spin Interactions. *J. Mol. Spectrosc.* **1991**, *148*, 371–377.
- 406 (42) Watson, J. K. G. In *Vibrational Spectra and Structure*; Durig, J. R.,  
407 Ed.; Elsevier: New York, 1977; Vol. 6, pp 1– 78.
- 408 (43) Gordy, W.; Cook, R. L. *Microwave Molecular Spectra*, 3rd ed.;  
409 Wiley: New York, 1984.
- 410 (44) Saenger, W. *Nature (London)* **1979**, *279*, 343.
- 411 (45) Jeffrey, G. A. *An Introduction to Hydrogen Bonding*; Oxford  
412 University Press: New York, 1997.
- 413 (46) *The Weak Hydrogen Bond in Structural Chemistry and Biology*;  
414 IUCr Monographs on Crystallography, Vol. IX; Desiraju, G. R.,  
415 Steiner, T., Eds.; Oxford University Press: Oxford, 2001.
- 416 (47) Lee, K. T.; Sung, J.; Lee, K. J.; Park, Y. D.; Kim, S. K.  
417 Conformation-dependent ionization energies of L-phenylalanine.  
418 *Angew Chem., Int. Ed.* **2002**, *41*, 4114–4117.
- 419 (48) Peña, I.; Cabezas, C.; Alonso, J. L. The Nucleoside Uridine  
420 Isolated in the Gas Phase. *Angew. Chem., Int. Ed.* **2015**, *10*, 2991–2994.